International Journal of Control, Automation and Systems 19(2) (2021) 999-1012
http://dx.doi.org/10.1007/s12555-019-0926-3
ISSN:1598-6446 eISSN:2005-4092
http://www.springer.com/12555

Dynamic H_∞ Feedback Boundary Control for a Class of Parabolic Systems with a Spatially Varying Diffusivity

Yanjiu Zhou*, Baotong Cui, and Xuyang Lou

Abstract: The dynamic H_∞ feedback boundary control for a class of parabolic distributed parameter systems with a non-constant (spatially varying) diffusion rate is addressed in this paper. The observer-based controller is designed to deal with non-collocated sensors and actuators, and the H_∞ performance index is employed to tackle the influence of the external disturbance and measurement noise. The resulting closed-loop system is formed by the boundary actuation with the H_∞ control strategy, and the output feedback is designed from the domain-averaged and boundary-valued measurement, respectively. With the sufficient conditions of the linear matrix inequality that infer the stability of the system, the corresponding gains of observer and controller are solved. Numerical simulations are given to show the validity of the main results.

Keywords: Boundary dynamic feedback control, H_∞ performance index, linear matrix inequality, non-constant diffusion rate, parabolic system.

1. INTRODUCTION

The distributed parameter systems (DPSs) have gradually gained the attention of scholars and researchers. The primary cause is that the evolution of processes in real life is not only related to time but also concerning location. For example, the temperature of the high-speed space shuttle's cooling wing changes during the actual motion [1], the auto chain reaction of catalytic rods happens in a chemical reactor [2], and the crowd evacuation is conducted when there appear congestions [3], etc. Besides, in the field of artificial intelligence control, some mechanical motion studies use DPSs for modeling and control operations. Gao *et al*. [4] developed the neural network controller for the two-link flexible manipulator to track the desired trajectory and suppress the flexible vibration, and in this process, partial differential equation (PDE) converted ordinary differential equation (ODE) via the assumed mode method. Whereafter, He *et al*. [5] utilized PDEs and ODEs to describe the system of a two-link rigid-flexible wing, retrained the vibrations, and achieved the desired angular position of the wing with boundary control. He *et al*. [6] also modeled a DPS coupling in bending and twisting to address a flexible micro aerial vehicle under spatiotemporally varying disturbances, along with two iterative learning control laws are designed to suppress the vibrations, reject the disturbances and regulate the displacement. Han *et al*. [7] investigate the robust control problem for a planar two-link rigid-flexible coupling manipulator using the sliding model control to control the joint angles, suppress the vibration and restrain the input disturbances simultaneously. DPSs can be described by PDEs, integral equations or partial-integral differential equations (PIDEs) [8]. Up to now, various issues concerning DPSs have been investigated, such as controllability and observability [9, 10], parameter identification [11, 12], filter design [13, 14], estimation and observation [15], controller design [16], deep learning algorithms to solve PDEs forward [17] and iterative learning control [18, 19], the problem of stabilization [20]. In addition, many scholars have made huge contributions to the research concerning parabolic systems. Hong *et al*. considered the adaptive control for parabolic systems, including direct control [21] and model reference control [22]. Applications to adaptive systems were also conducted when analyzing asymptotic behavior of coupled time-varying PDE system [23]. Recently, Li *et al*. [24] utilized the distributed effect of uncertain diffusion-dominated actuator dynamics to realize the adaptive stabilization of the ODE system. Adaptive control was also considered to stabilize a class of uncertain coupled parabolic system [25].

Manuscript received November 4, 2019; revised February 29, 2020 and May 3, 2020; accepted May 24, 2020. Recommended by Associate Editor Wei He under the direction of Editor-in-Chief Keum-Shik Hong. This work is supported by China Postdoctoral Science Foundation (2018M642160) and the 111 Project (B12018).

Yanjiu Zhou is with the Key Laboratory of Advanced Process Control for Light Industry (Ministry of Education), Jiangnan University, No. 1800 Lihu Avenue, Wuxi 214122, P. R. China (e-mail: zhouyanjiu99@163.com), and also with the Department of Chemical and Materials Engineering, University of Alberta, Edmonton, Alberta, T6G 2V4, Canada (e-mail: yanjiu@ualberta.ca). Baotong Cui and Xuyang Lou are with the Key Laboratory of Advanced Process Control for Light Industry (Ministry of Education), Jiangnan University, No. 1800 Lihu Avenue, Wuxi 214122, P. R. China (e-mails: {btcui, Louxy}@jiangnan.edu.cn).
* Corresponding author.

In the field of the control problem for the parabolic DPSs, the case of the constant diffusion rate is often considered for simplicity [26–28]. In fact, the diffusion rate varies with space, which means the diffusion rates at different locations are inconsistent, which can be seen in the inhomogeneous medium. The case of non-constant diffusivity is introduced into various control problems, such as the boundary controller design. Kerschbaum *et al*. [29] discussed coupled linear parabolic PDEs with space and time-dependent coefficients by the backstepping method. And even in the field of fractional order DPSs, Chen *et al*. [30, 31] considered the boundary control for the space-dependent fractional diffusion system. Besides, for perturbations, Fridman *et al*. [32, 34, 35] obtained many results concerning H_∞ control. And recently, the delayed H_∞ control under delayed point-like measurement was proposed by Selivanov and Fridman [36]. Liu *et al*. extended the H_∞ control problem to the stochastic reaction-diffusion systems with the mean square finite-time boundary stabilization. Motivated by the above results, the spatially varying diffusivity and the H_∞ control strategy are studied in this paper.

For the placement of the controller, the distributed control and boundary control are two different ways. The boundary actuation may have more conveniences when the space constraints and actuator limits are imposed. In real applications, measurement and execution may not be performed in the same place due to environmental constraints and operational difficulties. Sensors and actuators do not fit together, i.e., non-collocation of sensors and actuators. Hence, an observer is employed to estimate information that needed to be used in system control [37]. The method of measurement also plays a significant role. In the process, sensors are used to measure information and actuators to perform operations. Two measurement methods, the domain-averaged and boundary-valued are different due to the source of information data. The domain-averaged measurement includes all state information [38]. For the boundary-valued measurement, only the states at the boundary are obtained. This paper constructs the boundary controllers via the domain-averaged and boundary-valued measurement for the one-dimensional parabolic DPS (One-dimensional here refers to one-dimensional space).

In fact, many plants, such as the heat transfer process [39], fluid flow, and chemical reactor processes [2], are often described as models with disturbances and noise caused by the real-world environment. To deal with this case, various control approaches are proposed and employed, such as the slide model control [40, 41] and robust control [42, 43]. H_∞ control is also an important strategy [44]. Fridman *et al*. [32] designed the H_∞ static output feedback boundary controller for semi-linear parabolic systems with the space-dependent diffusivity. Wang *et al*. [37] discussed the boundary control via the measurement methods of the domain-averaged and boundary-valued. Inspired by the above literature, we further consider the H_∞ dynamic output feedback boundary control based on the observer design for the parabolic systems through the domain-averaged and boundary-valued measurement. Our objective is to provide a convenient and effective method based on linear matrix inequalities (LMIs) to solve the boundary control problem of parabolic systems with a spatially varying diffusion rate and the perturbation (the external disturbance and measurement noise are included). The main contributions of this paper can be presented as follows:

- To be more realistic and consistent with usual practical engineering processes, we consider the perturbation, including the external disturbance and measurement noise. Consequently, the H_∞ performance index is applied to deal with the disturbance and measurement noise, and so the corresponding H_∞ controller is designed in this paper.
- Two measurement methods are applied in the feedback. Firstly, the domain-averaged measurement is considered to get the related output, which is used to design an observer. This method obtains much information from the considered plant, which covers the whole space domain. And then, the second method, only the boundary information is utilized, which is also considered to design observers and address the dynamic H_∞ feedback boundary control problem of DPSs. It is called the boundary-valued measurement and the sensor is only placed at the boundary $x = 0$ in this paper.
- Observers are designed to deal with the case of non-collocated sensors and actuators. The feedback from observers will be used to construct effective controllers and they are only available at the boundary since the boundary control may be more suitable and could work better when no enough operating space and conditions are provided.

The further aim of this paper is to design H_∞ boundary controllers based on observers to reduce the influence that resulted from the external disturbance and measurement noise. For clear logic of our expression procedure, firstly, we give the process of the observer design in Section 3. And then in Section 4, we construct the boundary controller based on the related observer; the external disturbance and output measurement noise are considered, so the H_∞ performance index is introduced and the corresponding controller is implemented.

Meanwhile, two methods, i.e., the domain-averaged and boundary-valued measurement are employed to form the observer. Numerical simulations are provided in Section 5 to illustrate the effectiveness of the theoretical results obtained in the previous sections. Finally, Section 6 presents brief conclusions to this paper and some future work is drawn in.

2. PROBLEM FORMULATION AND PRELIMINARIES

Some mathematical notations to be used in this paper are given below. Let $\mathcal{R}$ define a set of real numbers. $\mathcal{H} = L_2(0,l)$ is Hilbert space, and then the norm of the square integrable function $\omega(x), x \in [0,l]$ is $\|\omega(x)\|_{L_2} = \sqrt{\int_0^l \omega^2(x)\,\mathrm{d}x}$. $\mathcal{S}^1(0,l)$ denotes a Sobolev space of absolutely continuous scalar functions $\omega(x)$ with $\omega(x) : [0,l] \to \mathcal{R}$, and $\frac{\mathrm{d}\omega}{\mathrm{d}x} \in L_2(0,l)$. $\mathcal{S}^2(0,l)$ denotes a Sobolev space of absolutely continuous scalar functions $\omega(x)$ with $\omega(x)$: $[0,l] \to \mathcal{R}$, $\frac{\mathrm{d}\omega}{\mathrm{d}x}$ is absolutely continuous and $\frac{\mathrm{d}^2\omega}{\mathrm{d}x^2} \in L_2(0,l)$. In this paper, $l > 0$ is a finite real number. The superscript T represents the transpose of a vector. The symmetric elements in the symmetric matrix are denoted by *.

Consider a class of diffusion systems in the following form:

$$z_t(x,t) = \frac{\partial}{\partial x}\left[a(x)\frac{\partial}{\partial x}z(x,t)\right] + r_0 z(x,t) + r_1 z(l,t), \quad x \in (0,l), \ \ t \in (0,+\infty), \tag{1}$$

with the initial condition

$$z(x,0) = z_0(x), \ \ x \in [0,l], \tag{2}$$

and subject to mixed boundary conditions

$$z_x(0,t) = 0 \ \ (\text{or } z(0,t) = 0), \ \ t \in (0,+\infty), \tag{3}$$

$$z_x(l,t) + qz(l,t) = 0, \ \ t \in (0,+\infty), \tag{4}$$

where $z(x,t)$ is the state variable of the system, $x \in [0,l]$ denotes the spatial position and $t \in [0,\infty)$ denotes the time. $z_t(x,t) = \frac{\partial z(x,t)}{\partial t}$, $\frac{\partial z(x,t)}{\partial x} = z_x(x,t)$. $a(x)$ is the diffusion rate, $a(x) \in \mathcal{C}^1[0,l]$ and $a(x) \geq a_{\min} > 0$, here $a_{\min}$ is a constant. r_0 is the reaction coefficient. $z(l,t)$ occurs in the system equation and it captures features of thermal instability in solid propellant rockets when $r_1 \neq 0$. The boundary condition at $x = 0$ can be Neumann type $z_x(0,t) = 0$ or Dirichlet $z(0,t) = 0$. The coefficients l and q in the boundary condition (4) are finite positive real numbers.

Remark 1: The above system describes the propagation of heat in a one-dimensional rod when $r_1 z(l,t) = 0$. And $z(l,t)$ is the boundary value presents the deviation from the steady-state when it is affected by the boundary value. The related study of solid propellant rockets can be seen in [32, 33].

3. OBSERVER DESIGN

3.1. Observer system

Firstly, we consider the domain-averaged measurement as the way to collect information. It means the data information obtained from the sensor is an averaged value of the whole space domain. The form of corresponding measurement equation is as follows:

$$y_{\text{out}}(t) = \frac{1}{l}\int_0^l z(x,t)\,\mathrm{d}x, \ \ t \in [0,+\infty). \tag{5}$$

Then, a Luenberger-type distributed parameter observer for the system (1)-(4) with the measurement equation (5) is designed as follows

$$\begin{cases} \hat{z}_t(x,t) = \dfrac{\partial}{\partial x}\left[a(x)\dfrac{\partial}{\partial x}\hat{z}(x,t)\right] + r_0\hat{z}(x,t) + r_1\hat{z}(l,t) \\ \qquad + \rho\left[y_{\text{out}}(t) - \hat{y}_{\text{out}}(t)\right], \\ \qquad x \in (0,l), t \in (0,+\infty), \\ \hat{z}_x(0,t) = 0, \ \ t \in (0,+\infty), \\ \hat{z}_x(l,t) + q\hat{z}(l,t) = 0, \ \ t \in (0,+\infty), \\ \hat{z}(x,0) = \hat{z}_0(x), \ \ x \in [0,l], \end{cases} \tag{6}$$

where $\rho > 0$ is an observer gain to be determined and the output of the observer is $\hat{y}_{\text{out}}(t) = \frac{1}{l}\int_0^l \hat{z}(x,t)\,\mathrm{d}x$.

Our objective is to find ρ such that state of the designed observer $\hat{z}$ converges to the state of considered plant z. Thus, we introduce the error variables $e \overset{\triangle}{=} z - \hat{z}$, which denotes the difference between the observer system and state system. And we expect this error converging to zero.

$$\begin{cases} e_t(x,t) = \dfrac{\partial}{\partial x}\left[a(x)\dfrac{\partial}{\partial x}e(x,t)\right] + r_0 e(x,t) + r_1 e(l,t) \\ \qquad - \rho\left[y_{\text{out}}(t) - \hat{y}_{\text{out}}(t)\right], \\ \qquad x \in (0,l), t \in (0,+\infty), \\ e_x(0,t) = 0, \ \ t \in (0,+\infty), \\ e_x(l,t) + qe(l,t) = 0, \ \ t \in (0,+\infty), \\ e(x,0) = e_0(x), \ \ x \in [0,l], \end{cases} \tag{7}$$

and $e_0(x) = z_0(x) - \hat{z}_0(x)$.

Here, the above error PDE can be rewritten as the evolution equation

$$\dot{e}(t) = \mathcal{A}e(t) + F(e(t)) - \rho\left[y_{\text{out}}(t) - \hat{y}_{\text{out}}(t)\right], \ t \geq 0, \tag{8}$$

in the Hilbert space $\mathcal{H} = L_2(0,l)$, the infinitesimal operator $\mathcal{A} = \frac{\partial\left[a(x)\frac{\partial}{\partial x}\right]}{\partial x}$ possesses the dense domain

$$\mathcal{D} = \{e \in \mathcal{H}^2(0,l) : e_x(0) = 0, e_x(l) + qe(l) = 0\}, \tag{9}$$

and $F(e(t)) = r_0 e(x,t) + r_1 e(l,t)$.

Similar to [32], the infinitesimal operator $\mathcal{A}$ generates an exponential semi-group $T(t)$, the corresponding norm satisfies $\|T(t)\|_{L_2} \leq \mu\exp(-\kappa t)$ everywhere with the constant $\mu > 0$ and decay rate $\kappa > 0$. It can be further concluded that the differential equation (8) with the domain (9) has a unique solution for any $t \geq 0$ according to Theorem 3.1.3 in Chapter 3 on Page 103 of [45].

3.2. Stability analysis

Next, we present our first main result on the stability of the error system. For the sake of the illustration of the theorem later, here we give an essential lemma that is needed in the subsequent proof.

Lemma 1 [35]**:** Let $z \in \mathcal{S}^1(0,l)$ is a scalar function, then

$$\int_0^l [z(x)-z(\zeta)]^2\,\mathrm{d}x \le \frac{l^2}{\pi^2}\int_0^l \left[\frac{\mathrm{d}z(x)}{\mathrm{d}x}\right]^2 \mathrm{d}x,$$

where $z(c) \triangleq \frac{1}{l}\int_0^l z(x)\,\mathrm{d}x$, $c \in (0,l)$ is a real number.

Theorem 1: The observer error system (7) is exponentially stable in the sense of $\|\cdot\|_{L_2}$ if there exists $\rho > 0$ such that

$$\begin{bmatrix} -\frac{\pi^2}{l^2}a_{\min}+r_0 & \frac{1}{2}r_1 & \frac{\pi^2}{l^2}a_{\min} \\ \frac{1}{2}r_1 & -\frac{qa(l)}{l} & 0 \\ \frac{\pi^2}{l^2}a_{\min} & 0 & -\frac{\pi^2}{l^2}a_{\min}-\rho \end{bmatrix} < 0. \quad (10)$$

Proof: Consider the Lyapunov function

$$V_1(t) = \frac{1}{2}\int_0^l e^2(x,t)\,\mathrm{d}x,\ \ t \ge 0. \quad (11)$$

Differentiation of $V_1(t)$ with respect to time along the solution of the system (7) yields

$$\begin{aligned}\frac{\mathrm{d}V_1(t)}{\mathrm{d}t} &= \int_0^l e(x,t)e_t(x,t)\,\mathrm{d}x \\ &= \int_0^l e(x,t)\frac{\partial}{\partial x}\left[a(x)\frac{\partial}{\partial x}e(x,t)\right]\mathrm{d}x \\ &\quad + r_0\int_0^l e^2(x,t)\,\mathrm{d}x + r_1\int_0^l e(x,t)e(l,t)\,\mathrm{d}x \\ &\quad - \rho\int_0^l e(x,t)\left[\frac{1}{l}\int_0^l e(x,t)\,\mathrm{d}x\right]\mathrm{d}x,\ \ t\ge 0. \end{aligned} \quad (12)$$

Employing integration by parts, the first mean value theorem for definite integrals, Lemma 1 and according to the boundary conditions in the system (7), the above equality (12) can be transformed into the following inequality

$$\begin{aligned}\frac{\mathrm{d}V_1(t)}{\mathrm{d}t} &\le \left(-\frac{\pi^2}{l^2}a_{\min}+r_0\right)\int_0^l e^2(x,t)\,\mathrm{d}x \\ &\quad - \frac{qa(l)}{l}\int_0^l e^2(l,t)\,\mathrm{d}x + r_1\int_0^l e(x,t)e(l,t)\,\mathrm{d}x \\ &\quad - \left(\frac{\pi^2}{l^2}a_{\min}+\rho\right)\int_0^l e^2(m,t)\,\mathrm{d}x \\ &\quad + \frac{2\pi^2}{l^2}a_{\min}\int_0^l e(x,t)e(m,t)\,\mathrm{d}x,\ \ t\ge 0, \end{aligned} \quad (13)$$

where m means that there exists a point $m \in (0,l)$ such that $\frac{1}{l}\int_0^l e(x,t)\,\mathrm{d}x = e(m,t)$.

Set $\boldsymbol{E}(x,t) \triangleq [e(x,t), e(l,t), e(m,t)]^{\mathrm{T}}$, and the right side of (13) can be rewritten as $\int_0^l \boldsymbol{E}^{\mathrm{T}}(x,t)\boldsymbol{\Xi}\boldsymbol{E}(x,t)\,\mathrm{d}x$. The coefficient matrix $\boldsymbol{\Xi}$ is equivalent to the matrix in (10).

Therefore, the inequality (13) can be written as

$$\frac{\mathrm{d}V_1(t)}{\mathrm{d}t} \le \int_0^l \boldsymbol{E}^{\mathrm{T}}(x,t)\boldsymbol{\Xi}\boldsymbol{E}(x,t)\,\mathrm{d}x,\ \ t\ge 0. \quad (14)$$

Additionally, we can find an appropriate scalar ε that satisfies the following inequality

$$\boldsymbol{\Xi} + \frac{1}{2}\varepsilon\boldsymbol{I} \le 0. \quad (15)$$

Substituting (15) into (14), we can obtain

$$\begin{aligned}\frac{\mathrm{d}V_1(t)}{\mathrm{d}t} &\le -\frac{1}{2}\varepsilon\int_0^l \boldsymbol{E}^{\mathrm{T}}(x,t)\boldsymbol{E}(x,t)\,\mathrm{d}x \\ &\le -\varepsilon V_1(t),\ \ t\ge 0. \end{aligned} \quad (16)$$

From above analysis, we can conclude that the error system converges to zero exponentially, which means the designed observer can follow the state system. The proof is completed. □

4. DYNAMIC FEEDBACK BOUNDARY CONTROL

4.1. Boundary control based on an observer

Consider the system (1) with the conditions (2), (3) and the control input $u(t)$ to be designed at the boundary $x = l$,

$$z_x(l,t) + qz(l,t) = u(t),\ \ t \in (0,+\infty). \quad (17)$$

To overcome the difficulty caused by the non-collocation between the actuator and sensor, the output feedback control technique based on an observer is applied. The measurement equation is still considered as (5). Firstly, a Luenberger-type distributed parameter observer for the system (1)-(3) with (17) is designed as (6) but the the control input is placed at the boundary $x = l$, i.e.,

$$\hat{z}_x(l,t) + q\hat{z}(l,t) = u(t),\ \ t \in (0,+\infty). \quad (18)$$

Then, with the help of the above observer, we design the following control law

$$u(t) = -k\int_0^l \hat{z}(x,t)\,\mathrm{d}x,\ \ t \in [0,+\infty), \quad (19)$$

where $k > 0$ is a control gain to be determined.

The corresponding error system, which has the same form of the error equation as (7), is easily obtained. Moreover, (19) can be rewritten as $u(t) = -k\int_0^l [z(x,t) - e(x,t)]\,\mathrm{d}x$, $\forall t \in [0,+\infty)$.

Similar to the well-posedness analysis of the error system in Section 3, the controlled closed-loop coupled system described by the state system (1)-(3) with (17) and the error system (7) has a unique solution.

Now, we are in the position to present our main result on the stability of the closed-loop system consisting of the state system (1)-(3) with (17) and the error system (7) under the controller (19), i.e., $u(t) = -k\int_0^l \hat{z}(x,t)\,\mathrm{d}x = -k\int_0^l [z(x,t)-e(x,t)]\,\mathrm{d}x$, $\forall t \in [0,+\infty)$. A necessary lemma concerning some inequalities is introduced for the formula derivation in the stability analysis.

Lemma 2 (Wirtinger's inequality) [46]**:** If $z \in \mathcal{S}^1(0,l)$ is a scalar function with $z(0)=0$ or $z(l)=0$, then

$$\int_0^l z^2(x)\,\mathrm{d}x \le \frac{4l^2}{\pi^2}\int_0^l \left[\frac{\mathrm{d}z(x)}{\mathrm{d}x}\right]^2 \mathrm{d}x.$$

Remark 2: From the above inequality in Lemma 2, without the conditions such as $z(0)=0$ or $z(l)=0$, the variation of Wirtinger's inequality can be obtained

$$\int_0^l [z(x)-z(0)]^2\,\mathrm{d}x \le \frac{4l^2}{\pi^2}\int_0^l \left[\frac{\mathrm{d}z(x)}{\mathrm{d}x}\right]^2 \mathrm{d}x,$$
$$\int_0^l [z(x)-z(l)]^2\,\mathrm{d}x \le \frac{4l^2}{\pi^2}\int_0^l \left[\frac{\mathrm{d}z(x)}{\mathrm{d}x}\right]^2 \mathrm{d}x.$$

Theorem 2: The controlled closed-loop system (1)-(3) with (17) is exponentially stable in the sense of $\|\cdot\|_{L_2}$ if there exist $\rho_1>0$, $k>0$ and $p>0$ such that

$$\begin{bmatrix} -\frac{\pi^2}{4l^2}a_{\min}+r_0 & -\frac{1}{2}a(l)k+\frac{1}{2}r_1+\frac{\pi^2}{4l^2}a_{\min} & 0 & 0 & 0 \\ * & -\frac{qa(l)}{l}-\frac{\pi^2}{4l^2}a_{\min} & \frac{1}{2}a(l)k & 0 & 0 \\ * & * & -\frac{\pi^2}{l^2}pa_{\min}+pr_0 & \frac{\pi^2}{l^2}pa_{\min} & \frac{1}{2}pr_1 \\ * & * & * & -\rho_1-\frac{\pi^2}{l^2}pa_{\min} & 0 \\ * & * & * & * & -\frac{pqa(l)}{l} \end{bmatrix} < 0, \tag{20}$$

where the observer gain will be obtained by $\rho = \rho_1/p$.

Proof: Consider the Lyapunov function

$$V_2(t) = \frac{1}{2}\int_0^l z^2(x,t)\,\mathrm{d}x + \frac{1}{2}p\int_0^l e^2(x,t)\,\mathrm{d}x,\ \ t\ge 0. \tag{21}$$

Differentiation of $V_2(t)$ with respect to time along the solution of the system closed-loop system consisting of (1)-(3) with (17) and (7) yields, for $t\ge 0$,

$$\begin{aligned}\frac{\mathrm{d}V_2(t)}{\mathrm{d}t} &= \int_0^l z(x,t)z_t(x,t)\,\mathrm{d}x + p\int_0^l e(x,t)e_t(x,t)\,\mathrm{d}x \\ &= \int_0^l z(x,t)\frac{\partial}{\partial x}\left[a(x)\frac{\partial}{\partial x}z(x,t)\right]\mathrm{d}x + r_0\int_0^l z^2(x,t)\,\mathrm{d}x \\ &\quad + r_1\int_0^l z(x,t)z(l,t)\,\mathrm{d}x \\ &\quad + p\int_0^l e(x,t)\frac{\partial}{\partial x}\left[a(x)\frac{\partial}{\partial x}e(x,t)\right]\mathrm{d}x \\ &\quad + pr_0\int_0^l e^2(x,t)\,\mathrm{d}x + pr_1\int_0^l e(x,t)e(l,t)\,\mathrm{d}x \\ &\quad - p\rho\int_0^l e(x,t)\left[\frac{1}{l}\int_0^l e(x,t)\,\mathrm{d}x\right]\mathrm{d}x. \end{aligned} \tag{22}$$

Employing integration by parts and with the help of the first mean value theorem for definite integrals, Lemma 1, Lemma 2, Remark 2 and boundary conditions in the closed-loop system (1)-(3) with (17), the equality (22) can be transformed into the following inequality

$$\begin{aligned}\frac{\mathrm{d}V_2(t)}{\mathrm{d}t} &\le \left(-\frac{\pi^2}{4l^2}a_{\min}+r_0\right)\int_0^l z^2(x,t)\,\mathrm{d}x \\ &\quad - \left(\frac{\pi^2}{4l^2}a_{\min}+\frac{qa(l)}{l}\right)\int_0^l z^2(l,t)\,\mathrm{d}x \\ &\quad + \left(\frac{\pi^2}{2l^2}a_{\min}-a(l)k+r_1\right)\int_0^l z(x,t)z(l,t)\,\mathrm{d}x \\ &\quad - \left(\frac{\pi^2}{l^2}pa_{\min}-pr_0\right)\int_0^l e^2(x,t)\,\mathrm{d}x \\ &\quad - \frac{pqa(l)}{l}\int_0^l e^2(l,t)\,\mathrm{d}x + pr_1\int_0^l e(x,t)e(l,t)\,\mathrm{d}x \\ &\quad - \left(\frac{\pi^2}{l^2}pa_{\min}+p\rho\right)\int_0^l e^2(m,t)\,\mathrm{d}x \\ &\quad + \frac{2\pi^2}{l^2}pa_{\min}\int_0^l e(x,t)e(m,t)\,\mathrm{d}x \\ &\quad + a(l)k\int_0^l e(x,t)z(l,t)\,\mathrm{d}x,\quad t\ge 0. \end{aligned} \tag{23}$$

Therefore, the inequality (23) can be written as

$$\frac{\mathrm{d}V_2(t)}{\mathrm{d}t} \le \int_0^l \boldsymbol{E}_{\mathbf{c}}^{\mathrm{T}}(x,t)\boldsymbol{\Xi}_{\mathbf{c}}\boldsymbol{E}_{\mathbf{c}}(x,t)\,\mathrm{d}x,\ \ t\ge 0, \tag{24}$$

where $\boldsymbol{E}_{\mathbf{c}}(x,t) \triangleq [z(x,t), z(l,t), e(x,t), e(m,t), e(l,t)]^{\mathrm{T}}$ and $\boldsymbol{\Xi}_{\mathbf{c}}$ is the matrix in (20).

Additionally, we can find an appropriate scalar ε_{c} that satisfies the following inequality

$$\boldsymbol{\Xi}_{\mathbf{c}} + \frac{1}{2}\varepsilon_{\mathrm{c}}\boldsymbol{I} \le 0. \tag{25}$$

Substituting (25) into (24), we can obtain

$$\begin{aligned}\frac{\mathrm{d}V_2(t)}{\mathrm{d}t} &\le -\frac{1}{2}\varepsilon_{\mathrm{c}}\int_0^l \boldsymbol{E}_{\mathbf{c}}^{\mathrm{T}}(x,t)\boldsymbol{E}_{\mathbf{c}}(x,t)\,\mathrm{d}x \\ &\le -\varepsilon_{\mathrm{c}}V_2(t),\ \ t\ge 0. \end{aligned} \tag{26}$$

From above analysis, we can conclude that the controlled closed-loop system consisting of (1)-(3) with (17) and (7) converges to zero exponentially, that means the designed controller (19) can stabilize the system exponentially. The proof is completed. □

4.2. H_∞ observer-based boundary control with domain-averaged measurement

To make the subsequent results more readable, a block diagram of the control system is presented as Fig. 1. The disturbance and noise in Fig. 1 often exit in the industrial process, and we should deal with them suitably to ensure the normal operation of the system. The controller based on an observer, together with H_∞ strategy is depicted in the blue block. When we address the system with perturbation, H_∞ control is a great choice because it can have a margin, which can be applied to different perturbations. In this paper, we employ the H_∞ control strategy and design the controller by using the maximum of the influence from the disturbance and noise.

Consider the perturbed version of the process (1)-(4)

$$\begin{cases} z_t(x,t) = \dfrac{\partial}{\partial x}\left[a(x)\dfrac{\partial}{\partial x}z(x,t)\right] + r_0 z(x,t) \\ \qquad + r_1 z(l,t) + bw(x,t), \\ \qquad x\in(0,l), t\in(0,+\infty), \\ z_x(0,t)=0, \ \ t\in(0,+\infty), \\ z_x(l,t)+qz(l,t)=u^{\mathrm{a}}(t), \ \ t\in(0,+\infty), \\ z(x,0)=z_0(x), \ \ x\in[0,l], \end{cases} \tag{27}$$

where $w(x,t)$ is an external disturbance with the related coefficient $b>0$ and $u^{\mathrm{a}}(t)$ is the control input at the boundary to be designed.

The measurement equation is considered as

$$y_{\mathrm{out}}^{\mathrm{a}}(t) = \frac{1}{l}\int_0^l z(x,t)\,\mathrm{d}x + v(t), \ \ t\in[0,+\infty), \tag{28}$$

where $v(t)$ is the noise that occurs in the measurement process, and the observed result doesn't contain any noise, which can be expressed as $\hat{y}_{\mathrm{out}}^{\mathrm{a}}(t) = \frac{1}{l}\int_0^l \hat{z}(x,t)\,\mathrm{d}x$, $\forall t\in[0,+\infty)$.

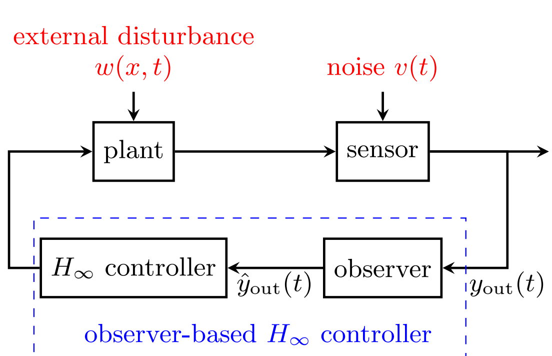

Fig. 1. Block diagram of the control system.

The corresponding observer system is written as

$$\begin{cases} \hat{z}_t(x,t) = \dfrac{\partial}{\partial x}\left[a(x)\dfrac{\partial}{\partial x}\hat{z}(x,t)\right] + r_0\hat{z}(x,t) + r_1\hat{z}(l,t) \\ \qquad + \rho_{\mathrm{h}}\{\dfrac{1}{l}\displaystyle\int_0^l [z(x,t)-\hat{z}(x,t)]\,\mathrm{d}x + v(t)\}, \\ \qquad x\in(0,l), t\in(0,+\infty), \\ \hat{z}_x(0,t)=0, \ \ t\in(0,+\infty), \\ \hat{z}_x(l,t)+q\hat{z}(l,t)=u^{\mathrm{a}}(t), \ \ t\in(0,+\infty), \\ \hat{z}(x,0)=\hat{z}_0(x), \ \ x\in[0,l], \end{cases} \tag{29}$$

where $\rho_{\mathrm{h}}>0$ is the observer gain to be determined.

The controller with the domain-averaged measurement is designed as

$$u^{\mathrm{a}}(t) = -k_{\mathrm{h}}\int_0^l \hat{z}(x,t)\,\mathrm{d}x, \ \ t\in[0,+\infty). \tag{30}$$

Similar to Section 3, the error system is derived as

$$\begin{cases} e_t(x,t) = \dfrac{\partial}{\partial x}\left[a(x)\dfrac{\partial}{\partial x}e(x,t)\right] + r_0 e(x,t) + r_1 e(l,t) \\ \qquad - \rho_{\mathrm{h}}\left[\dfrac{1}{l}\displaystyle\int_0^l e(x,t)\,\mathrm{d}x + v(t)\right] \\ \qquad + bw(x,t), \ \ x\in(0,l), t\in(0,+\infty), \\ e_x(0,t)=0, \ \ t\in(0,+\infty), \\ e_x(l,t)+qe(l,t)=0, \ \ t\in(0,+\infty), \\ e(x,0)=e_0(x), \ \ x\in[0,l]. \end{cases} \tag{31}$$

While stabilizing the above process (27), the external disturbance $w(x,t)$ has influences on the system state and controlled output as follows:

$$\bar{z}(x,t) = [\alpha(x,t,z)z(x,t), \ \ d(z(l,t),t)u^{\mathrm{a}}(t)]^{\mathrm{T}}, \tag{32}$$

where $\alpha(x,t,z)$ and $d(z(l,t),t)$ denote weight coefficients used to describe the extent to which the state of the system and controlled output is affected by the external disturbance. $\alpha(x,t,z)$ and $d(z(l,t),t)$ are continuous functions, which are uniformly bounded, i.e., $|\alpha(x,t,z)|\le\alpha_1$ and $|d(z(l,t),t)|\le d_1$ for all $(x,t,z)\in[0,l]\times[0,\infty)\times\mathcal{R}$, where $\alpha_1>0$, $d_1>0$. As the maximum of the influence, $\alpha_1>0$, $d_1>0$ will be utilized to form the equation of index J.

Thus, the H_∞ control problem is considered as follows. Given $\gamma_{\mathrm{h}}>0$, we need to find a dynamic output feedback controller (30) to stabilize the perturbed system (27). The negative performance index $J<0$ is considered as

$$J = \int_0^\infty\int_0^l \left[\bar{z}^{\mathrm{T}}(x,t)\bar{z}(x,t) - \gamma_{\mathrm{h}}^2 w^2(x,t) - \gamma_{\mathrm{h}}^2 v^2(t)\right]\mathrm{d}x\,\mathrm{d}t. \tag{33}$$

In order to solve the above problem, firstly, we study the condition that guarantees the following inequality

$$W(t) \triangleq \frac{\mathrm{d}V_2(t)}{\mathrm{d}t} + \int_0^l \left[\bar{z}^{\mathrm{T}}(x,t)\bar{z}(x,t) - \gamma_{\mathrm{h}}^2 w^2(x,t) - \gamma_{\mathrm{h}}^2 v^2(t)\right]\mathrm{d}x < 0,\ \ t \geq 0. \tag{34}$$

According to (32), and applying the the first mean value theorem for definite integrals, we can obtain

$$\begin{aligned}
&\int_0^l \bar{z}^{\mathrm{T}}(x,t)\bar{z}(x,t)\,\mathrm{d}x \\
&\leq \int_0^l \alpha_1^2 z^2(x,t)\,\mathrm{d}x + \int_0^l \int_0^l d_1^2 k_{\mathrm{h}}^2 \hat{z}^2(x,t)\,\mathrm{d}x\,\mathrm{d}x \\
&= \int_0^l \alpha_1^2 z^2(x,t)\,\mathrm{d}x + \int_0^l \int_0^l d_1^2 k_{\mathrm{h}}^2 [z(x,t) - e(x,t)]^2\,\mathrm{d}x\,\mathrm{d}x \\
&= \int_0^l \alpha_1^2 z^2(x,t)\,\mathrm{d}x + \int_0^l d_1^2 k_{\mathrm{h}}^2 l [z(x,t) - e(x,t)]^2\,\mathrm{d}x, \\
&t \geq 0.
\end{aligned} \tag{35}$$

Denoting

$$\begin{aligned}
\boldsymbol{E}_{\mathbf{h}}(x,t) = &[z(x,t), z(l,t), e(x,t), e(m,t), e(l,t), \\
&w(x,t), v(t)]^{\mathrm{T}},
\end{aligned}$$

and employing (23), we can get that

$$W(t) \leq \int_0^l \boldsymbol{E}_{\mathbf{h}}{}^{\mathrm{T}}(x,t)\boldsymbol{\Xi}_{\mathbf{h}}\boldsymbol{E}_{\mathbf{h}}(x,t)\,\mathrm{d}x < 0,\ \ t \geq 0, \tag{36}$$

if

$$\boldsymbol{\Xi}_{\mathbf{h}} \triangleq \begin{bmatrix}
\boldsymbol{\Xi}_{\mathbf{h}}^{\mathbf{11}} & \boldsymbol{\Xi}_{\mathbf{h}}^{\mathbf{12}} & \boldsymbol{\Xi}_{\mathbf{h}}^{\mathbf{13}} & 0 & 0 & \frac{1}{2}b & 0 \\
* & \boldsymbol{\Xi}_{\mathbf{h}}^{\mathbf{22}} & \boldsymbol{\Xi}_{\mathbf{h}}^{\mathbf{23}} & 0 & 0 & 0 & 0 \\
* & * & \boldsymbol{\Xi}_{\mathbf{h}}^{\mathbf{33}} & \frac{\pi^2}{l^2}pa_{\min} & \frac{1}{2}pr_1 & \frac{1}{2}pb & \boldsymbol{\Xi}_{\mathbf{h}}^{\mathbf{37}} \\
* & * & * & \boldsymbol{\Xi}_{\mathbf{h}}^{\mathbf{44}} & 0 & 0 & 0 \\
* & * & * & * & \boldsymbol{\Xi}_{\mathbf{h}}^{\mathbf{55}} & 0 & 0 \\
* & * & * & * & * & -\gamma_{\mathrm{h}}^2 & 0 \\
* & * & * & * & * & * & -\gamma_{\mathrm{h}}^2
\end{bmatrix} < 0, \tag{37}$$

where

$$\boldsymbol{\Xi}_{\mathbf{h}}^{\mathbf{11}} = -\frac{\pi^2}{4l^2}a_{\min} + r_0 + \alpha_1^2 + d_1^2 k_{\mathrm{h}}^2 l,\ \ \boldsymbol{\Xi}_{\mathbf{h}}^{\mathbf{13}} = -d_1^2 k_{\mathrm{h}}^2 l,$$

$$\boldsymbol{\Xi}_{\mathbf{h}}^{\mathbf{12}} = -\frac{1}{2}a(l)k_{\mathrm{h}} + \frac{1}{2}r_1 + \frac{\pi^2}{4l^2}a_{\min},\ \ \boldsymbol{\Xi}_{\mathbf{h}}^{\mathbf{23}} = \frac{1}{2}a(l)k_{\mathrm{h}},$$

$$\boldsymbol{\Xi}_{\mathbf{h}}^{\mathbf{22}} = -\frac{qa(l)}{l} - \frac{\pi^2}{4l^2}a_{\min},$$

$$\boldsymbol{\Xi}_{\mathbf{h}}^{\mathbf{33}} = -\frac{\pi^2}{l^2}pa_{\min} + pr_0 + d_1^2 k_{\mathrm{h}}^2 l,$$

$$\boldsymbol{\Xi}_{\mathbf{h}}^{\mathbf{44}} = -p\rho_h - \frac{\pi^2}{l^2}pa_{\min},\ \ \boldsymbol{\Xi}_{\mathbf{h}}^{\mathbf{55}} = -\frac{pqa(l)}{l},$$

$$\boldsymbol{\Xi}_{\mathbf{h}}^{\mathbf{37}} = -\frac{1}{2}p\rho_{\mathrm{h}}.$$

In order to obtain the feasible solution from the above nonlinear inequality (37), we need to linearize this nonlinear matrix inequality. By means of Schur complement, the following linear matrix inequality can be obtained:

$$\begin{bmatrix}
\boldsymbol{\Xi}_{\mathbf{h}}^{\mathbf{11}} - d_1^2 k_{\mathrm{h}}^2 l & \boldsymbol{\Xi}_{\mathbf{h}}^{\mathbf{12}} & 0 & 0 & 0 & \frac{1}{2}b & 0 & dk_{\mathrm{h}} \\
* & \boldsymbol{\Xi}_{\mathbf{h}}^{\mathbf{22}} & \Xi_{\mathrm{h}}^{23} & 0 & 0 & 0 & 0 & 0 \\
* & * & \boldsymbol{\Xi}_{\mathbf{h}}^{\mathbf{33}} - d_1^2 k_{\mathrm{h}}^2 l & \frac{\pi^2}{l^2}pa_{\min} & \frac{1}{2}pr_1 & \frac{1}{2}pb & -\frac{1}{2}\rho_{\mathrm{h}1} & -dk_{\mathrm{h}} \\
* & * & * & -\rho_{\mathrm{h}1} - \frac{\pi^2}{l^2}pa_{\min} & 0 & 0 & 0 & 0 \\
* & * & * & * & \boldsymbol{\Xi}_{\mathbf{h}}^{\mathbf{55}} & 0 & 0 & 0 \\
* & * & * & * & * & -\gamma_{\mathrm{h}}^2 & 0 & 0 \\
* & * & * & * & * & * & -\gamma_{\mathrm{h}}^2 & 0 \\
* & * & * & * & * & * & * & -\frac{1}{l}
\end{bmatrix} < 0, \tag{38}$$

where $\rho_{\mathrm{h}1} = p\rho_{\mathrm{h}}$.

Following the above analysis, we obtain the following result.

Theorem 3: Consider the perturbed system (27). Given $\gamma_{\mathrm{h}} > 0$, if there exists $p > 0$ such that the above LMI (38) is satisfied. Then the dynamic output feedback controller (30) with $k_{\mathrm{h}} > 0$ and the corresponding observer gain $\rho_{\mathrm{h}} > 0$ can stabilize the perturbed system (27), attenuates the disturbance $w(x,t)$ and noise $v(t)$ in the sense of (33).

Remark 3: In the case of Dirichlet type boundary condition at $x = 0$, i.e., $z(0,t) = 0$, the above results still effective because the product of $z(0,t)$ and $z_x(0,t)$ is still zero when $z(0,t) = 0$ or $z_x(0,t) = 0$ from computational point of view.

Remark 4: The above developed technique can be extended to the case of boundary-valued measurement. The differences from the domain-averaged measurement are that the boundary-valued one is only obtained from the value of the corresponding boundary state and the observer gain is injected into the boundary.

The implementations of the corresponding sensors have different ways. For the domain-averaged measurement, the only sensor collects the data information of its effective measurement range and the measured range is large enough to cover the whole space of the considered model system. The sensor is placed at the appropriate position, where one can collect information as much as possible, such as the central point. On the other hand, several sensors are placed in their respective effective ranges to obtain information. Then, through summarizing the information obtained by these sensors and then doing the average calculation, we can get the information of the domain-averaged measurement. For the boundary-valued measurement, the sensor is placed at the boundary. In this paper, the non-collocated situation is considered. The sensor is placed at the boundary $x = 0$, and the actuation is conducted at $x = l$. The effective range of the sensor is not required strictly since only the point value at the boundary $x = 0$ is collected, and the output of the observer $\hat{z}(x = l,t)$ is utilized. There are pros and cons to both ways. The domain-averaged measurement may obtain more information, including the whole space domain. The boundary-valued measurement only needs to get the boundary state but it may weaken the control effect. In this paper, we mainly focus on domain-averaged measurement and the related results on boundary-valued measurement are briefly given in Section 4.3.

4.3. H_∞ observer-based boundary control with boundary-valued measurement

In this section, we extend the design of the dynamic H_∞ boundary controller to the case of boundary-valued measurement from a theoretical perspective. The boundary-valued measurement equation is

$$y^{\mathrm{b}}_{\mathrm{out}} = z(0,t) + v_1(t), \;\; t \in [0,+\infty), \tag{39}$$

where $v_1(t)$ is the noise during the measurement process. It is presented different from $v(t)$ in (28) because the noise in the process is various according to the different methods of the measurement. And the observation used to correct the observer system is chosen as $\hat{y}^{\mathrm{b}}_{\mathrm{out}} = \hat{z}(0,t)$. Consequently, the corresponding observer can be designed as

$$\begin{cases} \hat{z}_t(x,t) = \dfrac{\partial}{\partial x}\left[a(x)\dfrac{\partial}{\partial x}\hat{z}(x,t)\right] + r_0\hat{z}(x,t) \\ \qquad\qquad + r_1\hat{z}(l,t), \;\; x \in (0,l), t \in (0,+\infty), \\ \hat{z}_x(0,t) = -\rho_{\mathrm{v}}[z(0,t) + v_1(t) - \hat{z}(0,t)], \\ \qquad\qquad t \in (0,+\infty), \\ \hat{z}_x(l,t) + q\hat{z}(l,t) = u^{\mathrm{b}}(t), \;\; t \in (0,+\infty), \\ \hat{z}(x,0) = \hat{z}_0(x), \quad x \in [0,l], \end{cases} \tag{40}$$

where ρ_{v} is the gain of the observer to be determined.

Then, we choose the observed value at the boundary $x = l$ as the feedback for the controller to be designed, and so the controller is presented as

$$u^{\mathrm{b}}(t) = -k_{\mathrm{v}}\hat{z}(l,t), \;\; t \in [0,+\infty). \tag{41}$$

One can obtain the following closed-loop system consisting of the state and error systems:

$$\begin{cases} z_t(x,t) = \dfrac{\partial}{\partial x}\left[a(x)\dfrac{\partial}{\partial x}z(x,t)\right] + r_0 z(x,t) \\ \qquad + r_1 z(l,t) + bw(x,t), \quad x \in (0,l), \\ \qquad t \in (0,+\infty), \\ z_x(0,t) = 0, \;\; t \in (0,+\infty), \\ z_x(l,t) + qz(l,t) = -k_{\mathrm{v}}[z(l,t) - e(l,t)], \\ \qquad t \in (0,+\infty), \\ z(x,0) = z_0(x), \;\; x \in [0,l], \\ e_t(x,t) = \dfrac{\partial}{\partial x}\left[a(x)\dfrac{\partial}{\partial x}e(x,t)\right] + r_0 e(x,t) \\ \qquad + r_1 e(l,t) + bw(x,t), \quad x \in (0,l), \\ \qquad t \in (0,+\infty), \\ e_x(0,t) = \rho_{\mathrm{v}}\left[e(0,t) + v_1(t)\right], \;\; t \in (0,+\infty), \\ e_x(l,t) + qe(l,t) = 0, \;\; t \in (0,+\infty), \\ e(x,0) = e_0(x), \;\; x \in [0,l]. \end{cases} \tag{42}$$

Similarly to Section 4.2, the closed-loop coupled system described by (42) has a unique solution and we can obtain the following theorem.

Theorem 4: Consider the perturbed system (42). Given $\gamma_{\mathrm{v}} > 0$, if there exist $p > 0$ and $0 < r < 1$ such that the following LMI (43) is satisfied. Then the dynamic output feedback controller (41) with $k_{\mathrm{v}} > 0$ and the corresponding observer gain $\rho_{\mathrm{v}} > 0$ can stabilize the perturbed system in (42) and attenuate the disturbance $w(x,t)$ and noise $v_1(t)$.

$$\begin{bmatrix} \boldsymbol{\Xi}^{11}_{\mathbf{v}} & \boldsymbol{\Xi}^{12}_{\mathbf{v}} & 0 & 0 & 0 & \boldsymbol{\Xi}^{16}_{\mathbf{v}} & 0 & 0 & 0 & 0 \\ * & \boldsymbol{\Xi}^{22}_{\mathbf{v}} + \frac{a(l)}{l}pk_{\mathrm{v}} - d_1^2k_{\mathrm{v}}^2 & 0 & 0 & 0 & 0 & 0 & \frac{a(l)}{2l}p & -k_{\mathrm{v}} & d_1k_{\mathrm{v}} \\ * & * & \boldsymbol{\Xi}^{33}_{\mathbf{v}} & \boldsymbol{\Xi}^{34}_{\mathbf{v}} & \boldsymbol{\Xi}^{35}_{\mathbf{v}} & \boldsymbol{\Xi}^{36}_{\mathbf{v}} & 0 & 0 & 0 & 0 \\ * & * & * & \boldsymbol{\Xi}^{44}_{\mathbf{v}} & 0 & 0 & \boldsymbol{\Xi}^{47}_{\mathbf{v}} & 0 & 0 & 0 \\ * & * & * & * & \boldsymbol{\Xi}^{55}_{\mathbf{v}} - d_1^2k_{\mathrm{v}}^2 & 0 & 0 & 0 & k_v & -d_1k_{\mathrm{v}} \\ * & * & * & * & * & \boldsymbol{\Xi}^{66}_{\mathbf{v}} & 0 & 0 & 0 & 0 \\ * & * & * & * & * & * & \boldsymbol{\Xi}^{77}_{\mathbf{v}} & 0 & 0 & 0 \\ * & * & * & * & * & * & * & -\sigma_0^{-1} & 0 & 0 \\ * & * & * & * & * & * & * & * & -\sigma_0 & 0 \\ * & * & * & * & * & * & * & * & * & -1 \end{bmatrix} < 0, \tag{43}$$

note that, to solve the above inequality, we choose $\sigma = \sigma_0$ as a known constant.

The detailed calculation for Theorem 4 is presented in Appendix A.

5. NUMERICAL SIMULATIONS

In this section, we provide numerical simulations to illustrate the effectiveness of the designed dynamic H_∞ boundary controller in Section 4.

The steps of our simulation are

- Firstly, we obtain the related gains of the observer and controller, i.e., the feasible solutions of LMI with the help of the YALMIP toolbox.
- Secondly, we construct the related controlled closed-loop systems (with the control input at the boundary $x = l$) of the state, observer, and error with the perturbation, the external disturbance and noise involved.
- Finally, we depict the corresponding figures, the effect of the designed controller is also analyzed.

We consider the body equation (1) corresponding to the initial condition (2) and boundary conditions (3)-(4), together with the spatially varying diffusivity $a(x) = 0.02(x-0.25)^2 + 1.8125$ (see Fig. 2). The other parameters of the system is considered as $r_0 = 0.5$, $r_1 = 2$, $q = 1.5$. The top limitation of the position variable in this paper is considered to be $l = 1$, so we conduct this numerical simulation in $x \in [0, l]$. And the simulation time T is set as $T = 10$ seconds, $t \in [0, T]$. The initial condition of the original system is set to be $z_0(x) = 0.25x(1-x)$ and the initial condition of the observer is $\hat{z}_0(x) = 0$, that is, the initial condition of the error system is $e_0(x) = 0.25x(1-x)$.

Furthermore, when we discuss the H_∞ dynamic boundary control, the system (27) with disturbance $w(x,t) = 0.05\cos(0.1x)\exp(-0.5t)$ and output measurement noise $v(t) = 0.9\sin(0.001t)\exp(-0.5t)$ is considered. Here we choose $\gamma_h = 1.95$. Moreover, some related parameters are chosen as follows: $b = 1$, $\alpha_1 = 1$, $d_1 = 0.1$.

The finite-difference approximation method and the way to estimate differential are adopted to solve the diffusion system. We choose the simulation time to be T seconds and divide T into m parts, i.e., the temporal step size is $\triangle t = T/m$ and there are $m+1$ grid points. The space is divided in the same way as time, i.e., $\triangle x = l/n$ and grid points are $n+1$. In this paper, $m = 6000$ and $n = 20$. It is worth noting that due to Robin condition (4), both the beginning and the end need to construct a virtual point to present the derivative respectively.

According to the above steps of this simulation, the corresponding actions and analyses are shown. Firstly, with the help of the YALMIP toolbox, we can obtain the feasible solutions $\rho_h = 5.9138$, $k_h = 1.8833$ in (38) and they will be subsequently employed to construct the observer system and the controller. The open-loop evolution of $z(x,t)$ with the external disturbance is shown in Fig. 3 and one can find that the uncontrolled system is unstable. Fig. 4 depicts the control input (30). The curve reaches zero gradually, which means the system has been stable and so no more control is needed. Fig. 5, Fig. 6 and Fig. 7 show the evolutions

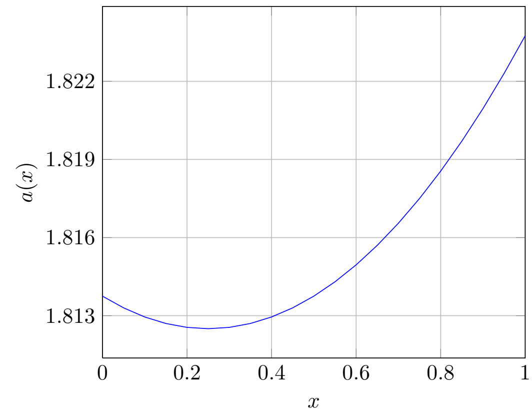

Fig. 2. Diffusivity $a(x)$.

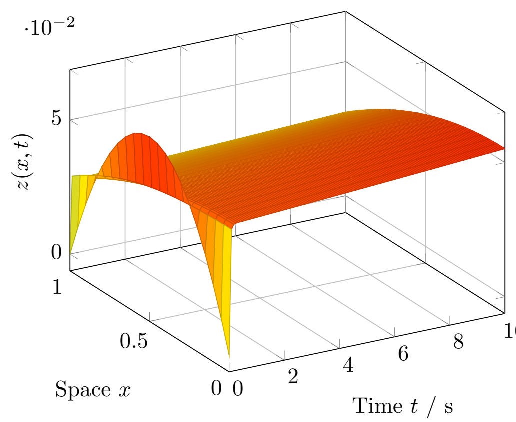

Fig. 3. Open-loop with perturbation.

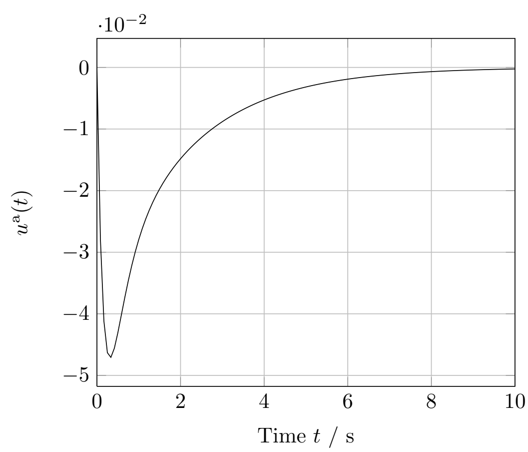

Fig. 4. Control input.

of closed-loop state system, observer system and error system respectively. One can see that the state of unstable system (27) gradually converge to zero under the boundary controller with domain-averaged measurement. The related L_2 norms of the above systems are shown in Fig. 8. The profiles of norms also imply that the controlled system is stable with the observer following the considered plant

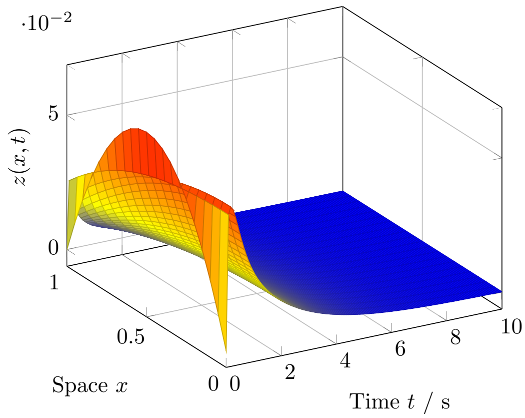

Fig. 5. Closed-loop state.

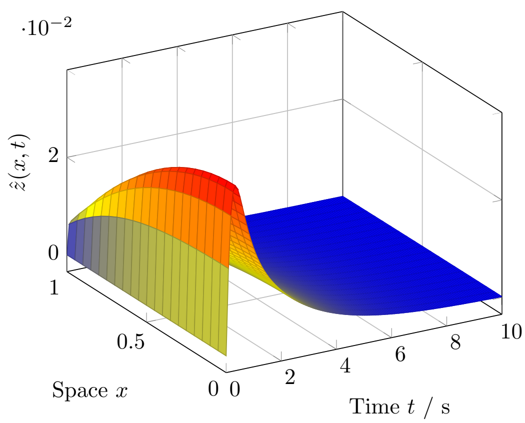

Fig. 6. Observer state.

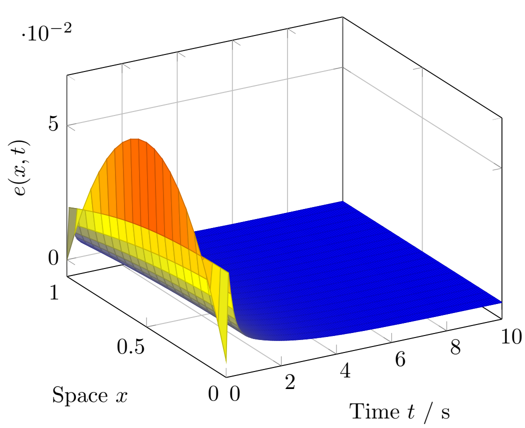

Fig. 7. The error $e(x,t)$.

quickly and accurately. Fig. 9 shows that $J<0$ satisfies the theoretical requirement. The index J is designed with the maximum of the influence brought from perturbation.

Remark 5: In this section, the backward difference method is utilized for the discretization of the parabolic system with a spatially varying diffusivity. This method can reduce the limitation for the related parameter adjustment caused by the strict grid ratio requirement compared with the forward difference method.

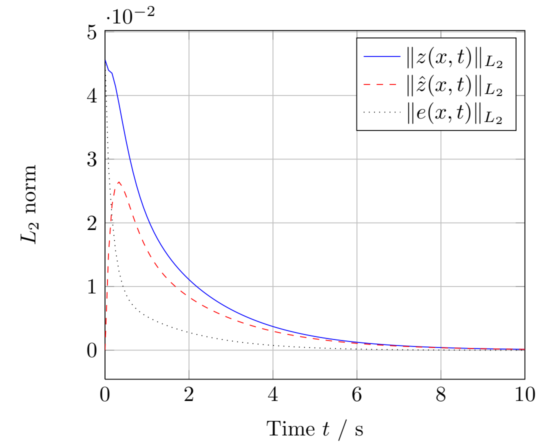

Fig. 8. L_2 norm.

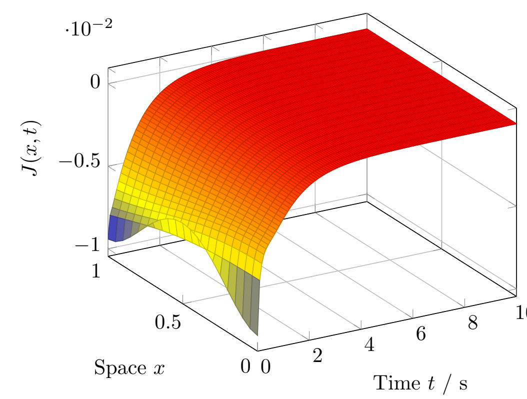

Fig. 9. Performance index J.

6. CONCLUSIONS

This paper has presented the H_∞ boundary control based on the observer for a class of DPSs with the spatially varying diffusivity. The external disturbance and measurement noise have been considered into the system model and the measurement equation, respectively. The observer has been employed to deal with non-collocated sensors and actuators. The controller is only active at the boundary $x=l$, which may be easier to implement, especially when the operating space and cost are limited. In the future, the H_∞ control problems for the more complex cases, such as the semi-linear, coupled and time-delayed systems, will be taken into consideration.

APPENDIX A

Consider the following Lyapunov function

$$V_3(t) = \frac{1}{2}p\int_0^l z^2(x,t)\,\mathrm{d}x + \frac{1}{2}\int_0^l e^2(x,t)\,\mathrm{d}x, \quad t\geq 0. \tag{A.1}$$

Through the calculations similar to Section 4.2, the differentiation of $V_3(t)$ with respect to time along the solution of the system (42) yields, for $t \geq 0$,

$$\begin{aligned}
\frac{\mathrm{d}V_3(t)}{\mathrm{d}t} &\\
\leq &\left(-\frac{\pi^2}{4l^2}a_{\min}+r_0\right)p\int_0^l z^2(x,t)\,\mathrm{d}x\\
&-\left(\frac{\pi^2}{4l^2}a_{\min}+\frac{qa(l)}{l}+\frac{a(l)}{l}k_{\mathrm{v}}\right)p\int_0^l z^2(l,t)\,\mathrm{d}x\\
&+\left(\frac{\pi^2}{2l^2}a_{\min}+r_1\right)p\int_0^l z(x,t)z(l,t)\,\mathrm{d}x\\
&+\left(r_0-\frac{\pi^2}{4l^2}a_{\min}\right)\int_0^l e^2(x,t)\,\mathrm{d}x\\
&-\left(\frac{a(0)}{l}\rho_{\mathrm{v}}+\frac{\pi^2}{4l^2}a_{\min}r\right)\int_0^l e^2(0,t)\,\mathrm{d}x\\
&-\left[\frac{qa(l)}{l}+\frac{\pi^2}{4l^2}a_{\min}(1-r)\right]\int_0^l e^2(l,t)\,\mathrm{d}x\\
&+\frac{\pi^2}{2l^2}a_{\min}r\int_0^l e(x,t)e(0,t)\,\mathrm{d}x\\
&+\left[\frac{\pi^2}{2l^2}a_{\min}(1-r)+r_1\right]\int_0^l e(x,t)e(l,t)\,\mathrm{d}x\\
&+\frac{a(l)}{l}pk_{\mathrm{v}}\int_0^l z(l,t)e(l,t)\mathrm{d}x+bp\int_0^l z(x,t)w(x,t)\mathrm{d}x\\
&-\frac{a(0)}{l}\rho_{\mathrm{v}}\int_0^l e(0,t)v_1(t)\,\mathrm{d}x+b\int_0^l e(x,t)w(x,t)\,\mathrm{d}x.
\end{aligned} \tag{A.2}$$

Consider the similar influence on the system state and controlled output as (32),

$$\bar{z}_1(x,t) = [\alpha(x,t,z)z(x,t),\ d(z(l,t),t)u^{\mathrm{b}}(t)]^{\mathrm{T}}, \tag{A.3}$$

and the similar negative performance index as (33), $J_1 < 0$ and

$$J_1 = \int_0^\infty\int_0^l\left[\bar{z}_1^{\mathrm{T}}(x,t)\bar{z}_1(x,t)-\gamma_{\mathrm{v}}^2w^2(x,t)-\gamma_{\mathrm{v}}^2v_1^2(t)\right]\mathrm{d}x\,\mathrm{d}t. \tag{A.4}$$

Then, to ensure the inequality

$$\begin{aligned}
M(t) \triangleq &\frac{\mathrm{d}V_3(t)}{\mathrm{d}t}\\
&+\int_0^l\left[\bar{z}_1{}^{\mathrm{T}}(x,t)\bar{z}_1(x,t)-\gamma_{\mathrm{v}}^2w^2(x,t)-\gamma_{\mathrm{v}}^2v_1^2(t)\right]\mathrm{d}x\\
<&0, \quad t\geq 0,
\end{aligned} \tag{A.5}$$

we require the following inequality holds

$$M(t) \leq \int_0^l \boldsymbol{E}_{\mathbf{v}}{}^{\mathrm{T}}(x,t)\boldsymbol{\Xi}_{\mathbf{v}}\boldsymbol{E}_{\mathbf{v}}(x,t)\,\mathrm{d}x < 0, \quad t\geq 0, \tag{A.6}$$

where

$$\boldsymbol{E}_{\mathbf{v}} = [z(x,t), z(l,t), e(x,t), e(0,t), e(l,t), w(x,t), v(t)]^{\mathrm{T}},$$

$$\boldsymbol{\Xi}_{\mathbf{v}} \triangleq \begin{bmatrix}
\boldsymbol{\Xi}_{\mathbf{v}}^{\mathbf{11}} & \boldsymbol{\Xi}_{\mathbf{v}}^{\mathbf{12}} & 0 & 0 & 0 & \boldsymbol{\Xi}_{\mathbf{v}}^{\mathbf{16}} & 0\\
* & \boldsymbol{\Xi}_{\mathbf{v}}^{\mathbf{22}} & 0 & 0 & \boldsymbol{\Xi}_{\mathbf{v}}^{\mathbf{25}} & 0 & 0\\
* & * & \boldsymbol{\Xi}_{\mathbf{v}}^{\mathbf{33}} & \boldsymbol{\Xi}_{\mathbf{v}}^{\mathbf{34}} & \boldsymbol{\Xi}_{\mathbf{v}}^{\mathbf{35}} & \boldsymbol{\Xi}_{\mathbf{v}}^{\mathbf{36}} & 0\\
* & * & * & \boldsymbol{\Xi}_{\mathbf{v}}^{\mathbf{44}} & 0 & 0 & \boldsymbol{\Xi}_{\mathbf{v}}^{\mathbf{47}}\\
* & * & * & * & \boldsymbol{\Xi}_{\mathbf{v}}^{\mathbf{55}} & 0 & 0\\
* & * & * & * & * & \boldsymbol{\Xi}_{\mathbf{v}}^{\mathbf{66}} & 0\\
* & * & * & * & * & * & \boldsymbol{\Xi}_{\mathbf{v}}^{\mathbf{77}}
\end{bmatrix}, \tag{A.7}$$

where

$$\begin{aligned}
\boldsymbol{\Xi}_{\mathbf{v}}^{\mathbf{11}} &= \left(r_0-\frac{\pi^2}{4l^2}a_{\min}\right)p+\alpha_1^2,\\
\boldsymbol{\Xi}_{\mathbf{v}}^{\mathbf{12}} &= \left(\frac{r_1}{2}+\frac{\pi^2}{4l^2}a_{\min}\right)p,\ \ \boldsymbol{\Xi}_{\mathbf{v}}^{\mathbf{16}} = \frac{b}{2}p,\\
\boldsymbol{\Xi}_{\mathbf{v}}^{\mathbf{22}} &= -\left(\frac{qa(l)}{l}+\frac{\pi^2}{4l^2}a_{\min}\right)p-\frac{a(l)}{l}pk_{\mathrm{v}}+d_1^2k_{\mathrm{v}}^2,\\
\boldsymbol{\Xi}_{\mathbf{v}}^{\mathbf{25}} &= \frac{a(l)}{2l}pk_{\mathrm{v}}-d_1^2k_{\mathrm{v}}^2,\ \ \boldsymbol{\Xi}_{\mathbf{v}}^{\mathbf{33}} = r_0-\frac{\pi^2}{4l^2}a_{\min},\\
\boldsymbol{\Xi}_{\mathbf{v}}^{\mathbf{34}} &= \frac{\pi^2}{4l^2}a_{\min}r,\ \ \boldsymbol{\Xi}_{\mathbf{v}}^{\mathbf{35}} = \frac{\pi^2}{4l^2}a_{\min}(1-r)+\frac{r_1}{2},\\
\boldsymbol{\Xi}_{\mathbf{v}}^{\mathbf{36}} &= \frac{1}{2}b,\ \ \boldsymbol{\Xi}_{\mathbf{v}}^{\mathbf{44}} = -\frac{\pi^2}{4l^2}a_{\min}r-\frac{a(0)}{l}\rho_{\mathrm{v}},\\
\boldsymbol{\Xi}_{\mathbf{v}}^{\mathbf{47}} &= -\frac{a(0)}{2l}\rho_{\mathrm{v}},\\
\boldsymbol{\Xi}_{\mathbf{v}}^{\mathbf{55}} &= -\frac{qa(l)}{l}-\frac{\pi^2}{4l^2}a_{\min}(1-r)+d_1^2k_{\mathrm{v}}^2,\\
\boldsymbol{\Xi}_{\mathbf{v}}^{\mathbf{66}} &= \boldsymbol{\Xi}_{\mathbf{v}}^{\mathbf{77}} = -\gamma_{\mathrm{v}}^2.
\end{aligned}$$

Next, we deal with the nonlinear quadratic terms pk_{v} in $\boldsymbol{\Xi}_{\mathbf{v}}^{\mathbf{22}}$ and $\boldsymbol{\Xi}_{\mathbf{v}}^{\mathbf{25}}$. $\boldsymbol{\Xi}_{\mathbf{v}}$ in (A.7) can be divided into two terms

$$\begin{bmatrix}
\boldsymbol{\Xi}_{\mathbf{v}}^{\mathbf{11}} & \boldsymbol{\Xi}_{\mathbf{v}}^{\mathbf{12}} & 0 & 0 & 0 & \boldsymbol{\Xi}_{\mathbf{v}}^{\mathbf{16}} & 0\\
* & \boldsymbol{\Xi}_{\mathbf{v}}^{\mathbf{22}}+\frac{a(l)}{l}pk_{\mathrm{v}} & 0 & 0 & \boldsymbol{\Xi}_{\mathbf{v}}^{\mathbf{25}}-\frac{a(l)}{2l}pk_{\mathrm{v}} & 0 & 0\\
* & * & \boldsymbol{\Xi}_{\mathbf{v}}^{\mathbf{33}} & \boldsymbol{\Xi}_{\mathbf{v}}^{\mathbf{34}} & \boldsymbol{\Xi}_{\mathbf{v}}^{\mathbf{35}} & \boldsymbol{\Xi}_{\mathbf{v}}^{\mathbf{36}} & 0\\
* & * & * & \boldsymbol{\Xi}_{\mathbf{v}}^{\mathbf{44}} & 0 & 0 & \boldsymbol{\Xi}_{\mathbf{v}}^{\mathbf{47}}\\
* & * & * & * & \boldsymbol{\Xi}_{\mathbf{v}}^{\mathbf{55}} & 0 & 0\\
* & * & * & * & * & \boldsymbol{\Xi}_{\mathbf{v}}^{\mathbf{66}} & 0\\
* & * & * & * & * & * & \boldsymbol{\Xi}_{\mathbf{v}}^{\mathbf{77}}
\end{bmatrix}
+\begin{bmatrix}
0 & 0 & 0 & 0 & 0 & 0 & 0\\
* & -\frac{a(l)}{l}pk_{\mathrm{v}} & 0 & 0 & \frac{a(l)}{2l}pk_{\mathrm{v}} & 0 & 0\\
* & * & 0 & 0 & 0 & 0 & 0\\
* & * & * & 0 & 0 & 0 & 0\\
* & * & * & * & 0 & 0 & 0\\
* & * & * & * & * & 0 & 0\\
* & * & * & * & * & * & 0
\end{bmatrix}. \tag{A.8}$$

The second matrix in (A.8) can be rewritten as

$$\begin{bmatrix} 0 \\ \frac{a(l)}{2l}p \\ 0 \\ 0 \\ 0 \\ 0 \\ 0 \end{bmatrix} \begin{bmatrix} 0 \\ -k_{\rm v} \\ 0 \\ 0 \\ k_{\rm v} \\ 0 \\ 0 \end{bmatrix}^{\rm T} + \begin{bmatrix} 0 \\ -k_{\rm v} \\ 0 \\ 0 \\ k_{\rm v} \\ 0 \\ 0 \end{bmatrix} \begin{bmatrix} 0 \\ \frac{a(l)}{2l}p \\ 0 \\ 0 \\ 0 \\ 0 \\ 0 \end{bmatrix}^{\rm T}$$

$$\leq \sigma \begin{bmatrix} 0 \\ \frac{a(l)}{2l}p \\ 0 \\ 0 \\ 0 \\ 0 \\ 0 \end{bmatrix} \begin{bmatrix} 0 \\ \frac{a(l)}{2l}p \\ 0 \\ 0 \\ 0 \\ 0 \\ 0 \end{bmatrix}^{\rm T} + \sigma^{-1} \begin{bmatrix} 0 \\ -k_{\rm v} \\ 0 \\ 0 \\ k_{\rm v} \\ 0 \\ 0 \end{bmatrix} \begin{bmatrix} 0 \\ -k_{\rm v} \\ 0 \\ 0 \\ k_{\rm v} \\ 0 \\ 0 \end{bmatrix}^{\rm T}, \quad \text{(A.9)}$$

where $\sigma > 0$. Then applying Schur complements to extend the dimension of matrix (A.7) and deal with the square terms $d_1^2 k_{\rm v}^2$ in $\boldsymbol{\Xi}_{\mathbf{v}}(22)$, $\boldsymbol{\Xi}_{\mathbf{v}}(25)$, and $\boldsymbol{\Xi}_{\mathbf{v}}(55)$, we have that (A.6) is equivalent to LMI (43).

REFERENCES

[1] B. Luo, H. N. Wu, and H. X. Li, "Adaptive optimal control of highly dissipative nonlinear spatially distributed processes with neuro-dynamic programming," *IEEE Trans. on Neural Networks and Learning Systems*, vol. 26, no. 4, pp. 684-696, May 2015.

[2] F. Logist and J. F. V. Impe, "Multiple objective optimisation of cyclic chemical systems with distributed parameters," *IFAC Proceedings Volumes*, vol. 42, no. 2, pp. 295-300, 2009.

[3] E. Cristiani, F. S. Priuli, and A. Tosin, "Modeling rationality to control self-organization of crowds: an environmental approach," *SIAM Journal on Applied Mathematics*, vol. 75, no. 2, pp. 605-629, January 2015.

[4] H. J. Gao, W. He, C. Zhou, and C. Y. Sun, "Neural network control of a two-link flexible robotic manipulator using assumed mode method," *IEEE Trans. on Industrial Informatics*, vol. 15, no. 2, pp. 755-765, February 2019.

[5] W. He, T. T. Wang, X. Y. He, L. J. Yang, and O. Kaynak, "Dynamical modeling and boundary vibration control of a rigid-flexible wing system," *IEEE/ASME Trans. on Mechatronics*, 2020. DOI: 10.1109/TMECH.2020.2987963

[6] W. He, T. T. Meng, X. Y. He, and C. Y. Sun, "Iterative learning control for a flapping wing micro aerial vehicle under distributed disturbances," *IEEE Trans. on Cybernetics*, vol. 49, no. 4, pp. 1524-1535, April 2019.

[7] F. M. Han and Y. M. Jia, "Sliding mode boundary control for a planar two-link rigid-flexible manipulator with input disturbances," *International Journal of Control, Automation and Systems*, vol. 18, no. 2, pp. 351-362, September 2019.

[8] S. Salsa, *Partial Differential Equations in Action From Modelling to Theory*, Springer, Milan, 2008.

[9] A. Shukla, N. Sukavanam, D. N. Pandey, and U. Arora, "Approximate controllability of second-order semilinear control system," *Circuits, Systems, and Signal Processing*, vol. 35, no. 9, pp. 3339-3354, September 2016.

[10] G. Q. Xu, "Necessary condition of linear distributed parameter systems with exact controllability," *Systems & Control Letters*, vol. 118, pp. 109-115, August 2018.

[11] S. Rudy, A. Alla, S. L. Brunton, and J. N. Kutz, "Data-driven identification of parametric partial differential equations," *SIAM Journal on Applied Dynamical Systems*, vol. 18, no. 2, pp. 643-660, January 2019.

[12] J. Chen, B. Jiang, and J. Li, "Missing output identification model based recursive least squares algorithm for a distributed parameter system," *International Journal of Control, Automation and Systems*, vol. 16, no. 1, pp. 150-157, February 2018.

[13] X. Lou and B. Cui, "Adaptive consensus filters for second-order distributed parameter systems using sensor networks," *Circuits, Systems, and Signal Processing*, vol. 34, no. 9, pp. 2801-2818, September 2015.

[14] M. A. Demetriou, "Spatial PID consensus controllers for distributed filters of distributed parameter systems," *Syst. Contr. Lett.* vol. 63, pp. 57-62, January 2014.

[15] Y. Jiang, C. Liu, Q. L. Zhang, and T. Y. Zhao, "Two side observer design for singular distributed parameter systems," *Systems & Control Letters* vol. 124, pp. 112-120, February 2019.

[16] W. Kang and E. Fridman, "Boundary constrained control of delayed nonlinear schrödinger equation," *IEEE Trans. on Automatic Control*, vol. 63, no. 11, pp. 3873-3880, January 2018.

[17] M. Raissi, P. Perdikaris, and G. E. Karniadakis, "Physics-informed neural networks: A deep learning framework for solving forward and inverse problems involving nonlinear partial differential equations," *Journal of Computational Physics*, vol. 278, pp. 686-707, February 2019.

[18] M. Hamidaoui, C. Shao, and S. Haouassi, "A PD-type iterative learning control algorithm for one-dimension linear wave equation," *International Journal of Control, Automation and Systems*, vol. 18, no. 4, pp. 1045-1052, 2020.

[19] Y.-H. Lan, J.-J. Xia, Y.-P. Xia, and P. Li, "Iterative learning consensus control for multi-agent systems with fractional order distributed parameter models," *International Journal of Control, Automation and Systems*, vol. 17, no. 11, pp. 2839-2849, November 2019.

[20] D.-X. Zhao, J.-J. Wang, and Y.-P. Guo, "The direct feedback control and exponential stabilization of a coupled heat PDE-ODE system with Dirichlet boundary interconnection," *International Journal of Control, Automation and Systems*, vol. 17, no. 1, pp. 38-45, January 2019.

[21] K.-S. Hong and J. Bentsman, "Direct adaptive control of parabolic systems: Algorithm synthesis, and convergence and stability analysis," *IEEE Trans. on Automatic Control*, vol. 39, no. 10, pp. 2018-2033, October 1994.

[22] K.-S. Hong and J. Bentsman, "Application of averaging method for integro-differential equations to model reference adaptive control of parabolic systems," *Automatica*, vol. 30, no. 9, pp. 1415-1419, September 1994.

[23] L.-S. Hong, "Asymptotic behavior analysis of a coupled time-varying system: Application to adaptive systems," *IEEE Trans. on Automatic Control*, vol. 42, no. 12, pp. 1693-1697, December 1997.

[24] J. Li and Y. G. Liu, "Adaptive stabilisation for a class of uncertain coupled parabolic equations," *International Journal of Control*, 2019. DOI: 10.1080/00207179.2018.1564842

[25] J. Li and Y. G. Liu, "Adaptive stabilization of ODE systems via distributed effect of uncertain diffusion-dominated actuator dynamics," *International Journal of Control*, vol. 92, no. 1, pp. 65-76, January 2019.

[26] J. W. Wang, "Observer-based boundary control of semi-linear parabolic PDEs with non-collocated distributed event-triggered observation," *Journal of the Franklin Institute*, vol. 356, no. 17, pp. 10405-10420, November 2019.

[27] J. W. Wang, Y. Q. Liu, and C. Y. Sun, "Observer-based dynamic local piecewise control of a linear parabolic PDE using non-collocated local piecewise observation," *IET Control Theory & Applications*, vol. 12, no. 3, pp. 346-358, January 2018.

[28] Y. Q. Liu, J. W. Wang, and C. Y. Sun, "Observer-based output feedback compensator design for linear parabolic PDEs with local piecewise control and pointwise observation in space," *IET Control Theory & Applications*, vol. 12, no. 13, pp. 1812-1821, September 2018.

[29] S. Kerschbaum and J. Deutscher, "Backstepping control of coupled linear parabolic PDEs with space and time dependent coefficients," *IEEE Trans. on Automatic Control*, vol. 65, no 7, pp. 3060-3067, 2020.

[30] J. Chen, B. T. Cui, and Y. Q. Chen, "Observer-based output feedback control for a boundary controlled fractional reaction diffusion system with spatially-varying diffusivity," *IET Control Theory & Applications*, vol. 12, no. 11, pp. 1561-1572, July 2018.

[31] J. Chen, B. T. Cui, and Y. Q. Chen, "Backstepping-based boundary control design for a fractional reaction diffusion system with a space-dependent diffusion coefficient," *ISA Trans.*, vol. 80, pp. 203-211, September 2018.

[32] E. Fridman and Y. Orlov, "An LMI approach to H_∞ boundary control of semilinear parabolic and hyperbolic systems," *Automatica*, vol. 45, no. 9, pp. 2060-2066, September 2009.

[33] D. M. Bošković and M. Krstić, "Stabilization of a solid propellant rocket instability by state feedback," *International Journal of Robust and Nonlinear Control*, vol. 13, no.5 , pp. 483-495, April 2003.

[34] E. Fridman and A. Blighovsky, "Robust sampled-data control of a class of semilinear parabolic systems," *Automatica*, vol. 48, no. 5, pp. 826-836, May 2012.

[35] E. Fridman and N. B. Am, "Sampled-data distributed H_∞ control of transport reaction systems," *SIAM Journal on Control and Optimization*, vol. 51, no. 2, pp. 1500-1527, January 2013.

[36] A. Selivanov and E. Fridman, "Delayed H_∞ control of 2D diffusion systems under delayed pointlike measurements," *Automatica*, vol. 109, 108541, November 2019.

[37] J. W. Wang, H. N. Wu, and C. Y. Sun, "Local exponential stabilization via boundary feedback controllers for a class of unstable semi-linear parabolic distributed parameter processes," *Journal of the Franklin Institute*, vol. 354, no. 13, pp. 5221-5244, September 2017.

[38] H. N. Wu, J. W. Wang, and H. X. Li, "Exponential stabilization for a class of nonlinear parabolic PDE systems via fuzzy control approach," *IEEE Trans. on Fuzzy Systems*, vol. 20, no. 2, pp. 318-329, October 2012.

[39] W. A. Hadad, D. Maillet, and Y. Jannot, "Modeling unsteady diffusive and advective heat transfer for linear dynamical systems: A transfer function approach," *International Journal of Heat and Mass Transfer*, vol. 115, pp. 304-313, December 2017.

[40] A. Pisano and Y. Orlov, "Boundary second-order sliding-mode control of an uncertain heat process with unbounded matched perturbation," *Automatica*, vol. 48, no. 8, pp. 1768-1775, August 2012.

[41] A. Baccoli, Y. Orlov, A. Pisano, and E. Usai, "Sliding-mode boundary control of a class of perturbed reaction-diffusion processes," *International Workshop on Recent Advances in Sliding Modes (RASM)*, Istanbul, Turkey, pp. 1-6, July 2015.

[42] A. Cristofaro, "Robust tracking control for a class of perturbed and uncertain reaction-diffusion equations," *IFAC Proceedings Volumes*, vol. 47, no. 3, pp. 11375-11380, August 2014.

[43] S. J. Ho and B. S. Chen, "Robust fuzzy H_∞ estimator-based stabilization design for nonlinear parabolic partial differential systems with different boundary conditions," *IEEE Trans. on Fuzzy Systems*, vol. 24, no. 1, pp. 208-222, July 2016.

[44] M. Chinnamuniyandi, R. Ramachandran, J. Cao, G. Rajchakit, and X. Li, "A new global robust exponential stability criterion for H∞ control of uncertain stochastic neutral-type neural networks with both timevarying delays," *International Journal of Control, Automation and Systems*, vol. 16, no. 2, pp. 726-738, April 2018.

[45] R. F. Curtain and H. Zwart, *An Introduction to Infinite-dimensional Linear Systems Theory*, Springer, New York, 1995.

[46] P. G. Hardy, J. E. Littlewood, and G. Pólya, *Inequalities*, Cambridge University Press, Cambridge, UK, 1934.

Yanjiu Zhou received her Bachelor's degree in electric information engineering from Nanjing Forestry University, Nanjing, China, in June 2016. From September 2016, she is pursuing a Ph.D. degree at Jiangnan University. She is currently a Joint Training Ph.D. Student at the Department of Chemical & Materials Engineering, University of Alberta, from June 2019. Her research interests include distributed parameter systems, boundary control, robust control and stability of dynamical systems.

Baotong Cui received his Ph.D. degree in control theory and control engineering from the College of Automation Science and Engineering, South China University of Technology, China in July 2003. He was a post-doctoral fellow at Shanghai Jiao-Tong University, China, from July 2003 to September 2005, and a visiting scholar at the Department of Electrical and Computer Engineering, National University of Singapore, Singapore, from August 2007 to February 2008. He became an associate professor in December 1993 and a full professor in November 1995 at the Department of Mathematics, Binzhou University, China. He joined Jiangnan University, China in June 2003, where he is a full professor for the School of IoT Engineering. His current research interests include systems analysis, control of distributed parameter systems, stability of dynamical systems, artificial neural networks, and chaos synchronization.

Xuyang Lou received his Ph.D. degree in control theory and control engineering from Jiangnan University, Wuxi, China, in 2009. In 2010, he joined the School of Communication and Control Engineering, Jiangnan University. From October 2007 to October 2008, he was a visiting scholar in the CSIRO Division of Mathematical and Information Sciences, Adelaide, Australia. From July to November 2010, he was a Postdoctoral Fellow in the Department of Electrical Engineering (ESAT-SCDSISTA), Katholieke Universiteit Leuven. From July 2014 to February 2015, he visited the Computer Engineering Department, University of California, Santa Cruz, USA. He is currently a Professor with Jiangnan University. His current research interests include hybrid systems, distributed parameter systems and computational intelligence.

Publisher's Note Springer Nature remains neutral with regard to jurisdictional claims in published maps and institutional affiliations.